Electronic Supplementary Information for

Nitrogen-doped star-shaped polycyclic aromatic hydrocarbons based on fused triazatruxenes: synthesis and optoelectronic properties

Cheng-Fang Liu,[a‡] Cheng Cheng,[a‡] Yi Jiang,[a] Wen-Yong Lai,*[a] and Wei Huang[ab]

[a] Key Laboratory for Organic Electronics and Information Displays (KLOEID), Institute of Advanced Materials (IAM), Jiangsu National Synergetic Innovation Center for Advanced Materials (SICAM), Nanjing University of Posts & Telecommunications, 9 Wenyuan Road, Nanjing 210023, China

[b] Shaanxi Institute of Flexible Electronics (SIFE), Northwestern Polytechnical University (NPU), 127 West Youyi Road, Xi'an 710072, Shaanxi, China

‡ These authors contributed equally to this work.

*Email: iamwylai@njupt.edu.cn (W.-Y. Lai)

1. Materials and general methods.

All the reagents used were purchased from Sigma-Aldrich, J&K or Xiya Reagent (China). When necessary, solvents and reagents were purified using standard procedures.

Microwave-assisted reactions were performed using a CEM Discovery single-mode focused microwave system. The pressure was controlled by a load cell connected to the vessel via the septum. The temperature of the contents of the vessel was monitored using a calibrated infrared temperature control mounted under the reaction vessel.

NMR spectra were recorded on a Bruker Ultra Shield Plus 400 MHz NMR (^{1}H: 400 MHz, ^{13}C: 100 MHz). The matrix assisted laser desorption ionization time of flight mass spectroscopy (MALDI-TOF MS) measurements were carried out with a Shimadzu AXIMA-CFR mass

spectrometer. UV-visible absorption spectra were recorded on a Shimadzu UV-3600. UV-VIS-NIR spectrophotometer photoluminescence (PL) spectra were measured using a RF-5301PC spectrofluorophotometer. Electrochemical behavior was investigated by cyclic voltammetry (CV) with a standard three-electrode electrochemical cell in a 0.1 M tetra-*n*-butylammonium hexafluorophosphate (Bu_4NPF_6) in nonaqueous acetonitrile at room temperature under nitrogen with a scanning rate of 50 mV/s. A platinum working electrode, a glassy carbon electrode, and an $Ag/AgNO_3$ (0.1 M) reference electrode were used. The CV curves were calibrated using ferrocene/ferrocenium (Fc/Fc^+) redox couple (4.8 eV below the vacuum level) as the internal standard. The formal potential of Fc/Fc^+ was measured as 0.09 V against Ag/Ag^+. Thus, the highest occupied molecular orbital (HOMO) could be calculated according to: $E_{HOMO} = -e(E_{ox} + 4.71\ V)$, where E_{ox} is the onset oxidation. For reduction processes that were irreversible, the LUMO levels were deduced from the HOMO and optical band gaps by: $E_{LUMO} = E_{HOMO} + E_g$. Differential scanning calorimetry (DSC) and thermo-gravimetric analysis (TGA) were done on Shimadzu DSC-60A and DTG-60A equipment, respectively. The molecular structures of the tetraindoles were optimized using density functional theory (DFT) method (B3LYP) with 6-31G (d) basis set by GAUSSIAN 09.[1]

2. Synthesis and characterization.

5,10,15-trihexyl-2,3,7,8,12,13-hexa(naphthalen-2-yl)-10,15-dihydro-5H-diindolo[3,2-a:3',2'-c]carbazole (TATNa). A solution of TATBr (100 mg, 0.074 mmol), naphthalen-2-ylboronic acid (114 mg, 0.66 mmol), Tetrabutyl ammonium bromide (TBAB) (14.2 mg, 0.044 mmol) and KOH (37.6 mg, 0.67 mmol) in THF (3 mL) in a 10 mL pressurized vessel was carefully degassed before and after the addition of [Pd $(PPh_3)_4$] (51.3 mg, 0.044 mmol). The vessel was sealed and heated in the CEM Discover system. The initial microwave power was set at 200 W. The temperature of the

reaction was monitored by using a calibrated infrared temperature control mounted under the reaction vessel. A load cell, connected to the vessel through the septum, controlled the pressure. After the set temperature of 150°C was reached, the microwave power regulated itself to keep that temperature for 30 min before cooling to room temperature (RT). The mixture was subsequently diluted with CH_2Cl_2 and then washed with a saturated solution of brine, dried (Na_2SO_4), and evaporated. The resulting residue was purified with column chromatography using hexane/CH_2Cl_2 as eluant to give the final product as a white solid (45 mg, 45%). ^{1}H NMR (400 MHz, $CDCl_3$): δ 8.46 (s, 2H), 8.24 (d, J = 22.7 Hz, 1H), 8.00 (s, 6H), 7.90 (s, 3H), 7.86–7.67 (m, 15H), 7.83-7.68 (m, 6H), 7.48-7.39 (d, J= 8.6 Hz, 9H), 7.34 (s, 6H), 2.18–2.05 (m, 6H), 1.03 (s, 5H), 0.86 (t, J = 21.9, 11.2 Hz, 16H), 0.57 (m, J = 11.5, 4.4 Hz, 7H). ^{13}C NMR (100 MHz, $CDCl_3$): δ 141.5, 140.7, 140.1, 133.5, 132.5, 128.2, 127.7, 125.7, 124.1, 119.5, 112.6, 112.4, 108.9, 103.0, 47.2, 31.6, 30.4, 29.8, 26.6, 22.3, 13.8. MS (MALDI-TOF, *m/z*) $[M]^+$ Calcd for $C_{102}H_{87}N_3$, 1354.69; Found: 1354.61. Anal.Calcd for $C_{102}H_{87}N_3$: C 90.43, H 6.47, N 3.10. Found: C 90.39, H 6.48, N 3.13.

TATNaC1. $FeCl_3$ (48 mg, 0.30 mmol) was placed in a two-necked flask and CH_3NO_2 (1.0 mL) was added. The $FeCl_3$ solution was purged with argon for 10 min and slowly transferred to a solution of TATNa (102 mg, 0.075 mmol) in CH_2Cl_2 (20 mL, purged with argon for 10 min). After the mixture was stirred at 0°C for 30 min, a saturated aqueous $NaHCO_3$ solution (20 mL) was added. The resulting organic phase was extracted with CH_2Cl_2 (50 mL), washed with water, and then dried over anhydrous Na_2SO_4. After the solvents were removed in vacum, the mixture was purified by silica gel column chromatography to give TATNaC1 (30 mg) in 30% yield as a faint yellow solid. ^{1}H NMR (400 MHz, $CDCl_3$): δ 8.50 (s, 2H), 8.22 (d, J = 1.9 Hz, 1H), 8.01 (d, J=12.2 Hz, 6H), 7.92 (d, J=16.4 Hz, 3H), 7.87 – 7.70 (m, 15H), 7.58 (s, 4H), 7.45 (s, 9H), 7.31 (d, J = 5.8 Hz, 6H), 5.00 (d, J=5.8 Hz, 6H), 2.15 (s, 6H), 1.05 (d, J = 6.9 Hz, 6H), 0.93 – 0.77 (m, 16H), 0.55 (m, J = 9.2, 5.5 Hz,

5H). ^{13}C NMR (100 MHz, $CDCl_3$): δ 135.9, 135.7, 132.6, 132.0, 131.8, 131.5, 129.7, 128.6, 127.8, 126.5, 126.3, 126.5 – 125.5, 125.4, 124.7, 124.1, 123.0, 122.1, 119.4, 112.6, 102.9, 46.6, 32.0, 31.3, 30.1, 29.1, 26.4, 26.1, 22.4, 13.8. MS (MALDI-TOF, *m/z*) $[M]^+$ Calcd for $C_{102}H_{85}N_3$, 1352.68; Found: 1352.58. Anal.Calcd for $C_{102}H_{85}N_3$: C 90.56, H 6.33, N 3.11. Found: C 90.54, H 6.32, N 3.14.

TATNaC2. Synthesis steps to TATNaC2 are the same as those for compound TATNaC1 except for the ratio of the catalyst. $FeCl_3$ (96 mg, 0.60 mmol) was placed in a two-necked flask and CH_3NO_2 (1 mL) was added. After 30 min, the reaction was quenched by saturated aqueous $NaHCO_3$ solution. The solvents were removed under vacuum and the precipitate was purified by column chromatography on silica gel to give TATNaC2 (35 mg, 35% yield) as a pale yellow solid. ^{1}H NMR (400 MHz, $CDCl_3$): δ 9.09 (d, J = 35.7 Hz, 2H), 8.47 (d, J = 11.8 Hz, 1H), 8.16 (s, 6H), 8.09 – 7.65 (m, 18H), 7.51 (s, 11H), 7.31 (s, 2H), 7.24 (s, 4H), 4.86 (s, 6H), 2.01 (d, J = 24.3 Hz, 6H), 1.55 (s, 6H), 1.07 (s, 12H), 0.56 (s, 9H). ^{13}C NMR (100 MHz, $CDCl_3$): δ 140.8, 132.2, 131.9, 129.7, 127.8, 126.6, 126.3, 125.9, 125.4, 120.6, 115.2, 115.1, 114.1, 102.8, 102.3, 32.0, 31.5, 30.3, 29.0, 22.4, 13.8. MS (MALDI-TOF, *m/z*) $[M]^+$ Calcd for $C_{102}H_{83}N_3$, 1350.66; Found: 1350.42. Anal.Calcd for $C_{102}H_{83}N_3$: C 90.70, H 6.19, N 3.11. Found: C 90.67, H 6.31, N 3.12.

TATNaC3. Synthesis steps to TATNaC3 are the same as those for compound TATNaC1 except for the ratio of the catalyst. $FeCl_3$ (144 mg, 0.90 mmol) was placed in a two-necked flask and CH_3NO_2 (1 mL) was added. After 30 min, the reaction was quenched by saturated aqueous $NaHCO_3$ solution. The solvents were removed under vacuum and the precipitate was purified by column chromatography on silica gel to give TATNaC3 (66 mg, 65% yield) as a yellow solid. ^{1}H NMR (400 MHz, $CDCl_3$): δ 9.04 (d, J = 6.2 Hz, 2H), 8.64 – 8.50 (m, 1H), 8.21 (d, J = 10.9 Hz, 6H), 7.90 (d, J = 41.3, 28.7 Hz, 15H), 7.53 (s, 9H), 7.33 (d, J = 4.0 Hz, 6H), 4.41 (d, J = 46.0 Hz, 6H), 1.76 (s,

6H), 1.56 (d, J = 10.2 Hz, 6H), 1.36 (s, 12H), 0.58 – 0.35 (m, 9H). ^{13}C NMR (100 MHz, $CDCl_3$): δ 135.8, 133.5, 132.0, 129.3, 129.2, 128.3, 127.7, 127.7, 127.2, 126.0, 125.5, 123.0, 122.8, 112.9, 112,3, 103.1, 47.2, 31.6, 30.6, 29.9, 29.6, 29.0, 13.8. MS (MALDI-TOF, *m/z*) $[M]^+$ Calcd for $C_{102}H_{81}N_3$, 1348.65; Found: 1348.35. Anal.Calcd for $C_{102}H_{81}N_3$: C 90.83, H 6.05, N 3.12. Found: C 90.79, H 6.07, N 3.14.

MALDI-TOF and NMR spectra.

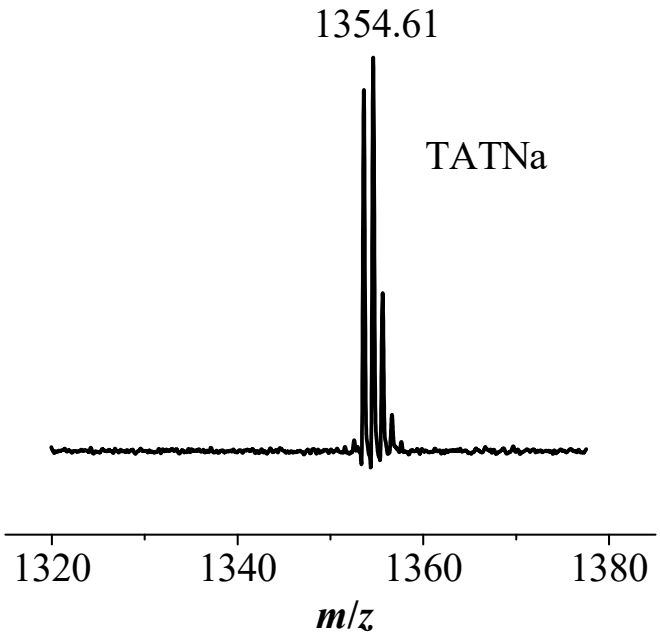

Figure S1. MALDI-TOF MS of TATNa

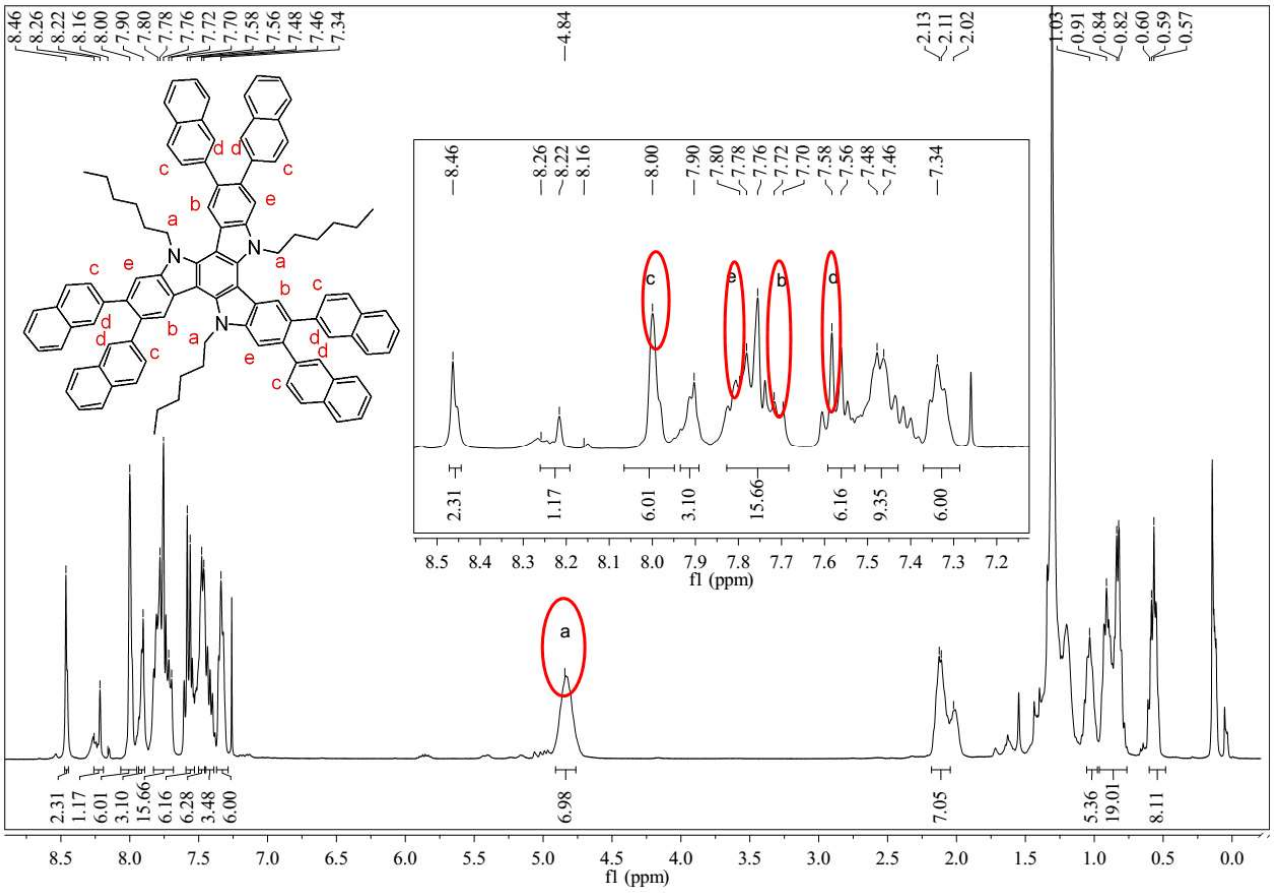

Figure S2. ^{1}H NMR spectra of TATNa

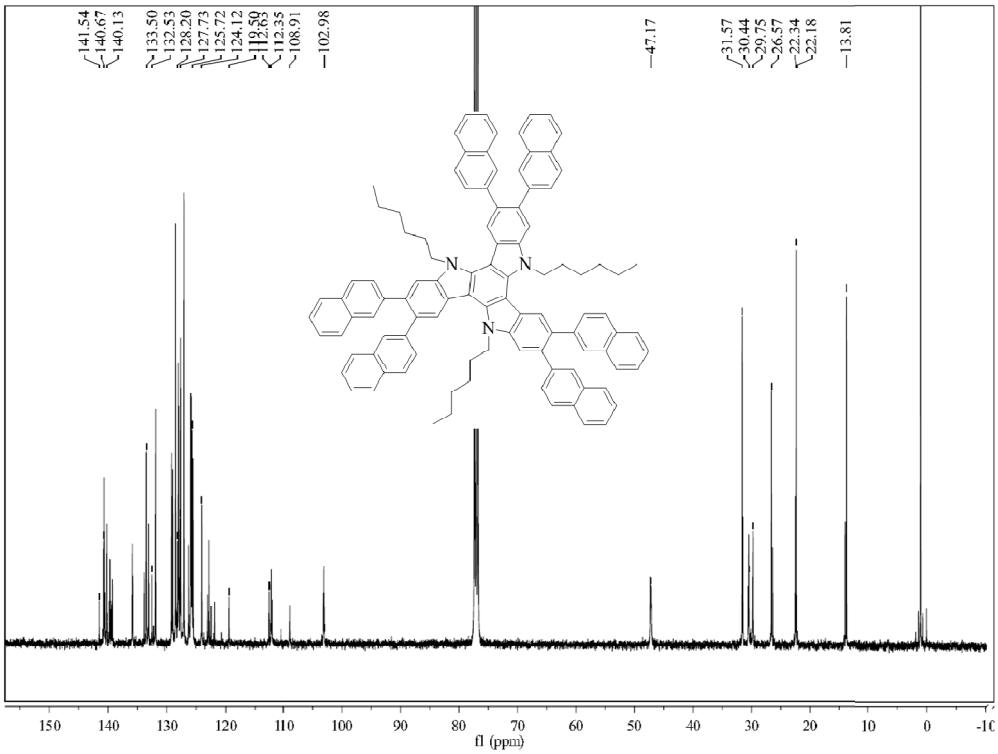

Figure S3. ^{13}C NMR spectra of TATNa

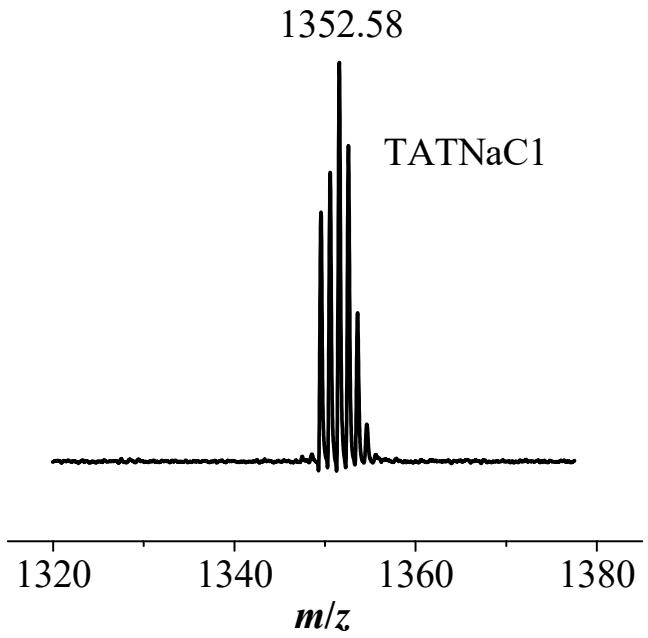

Figure S4. MALDI-TOF MS of TATNaC1

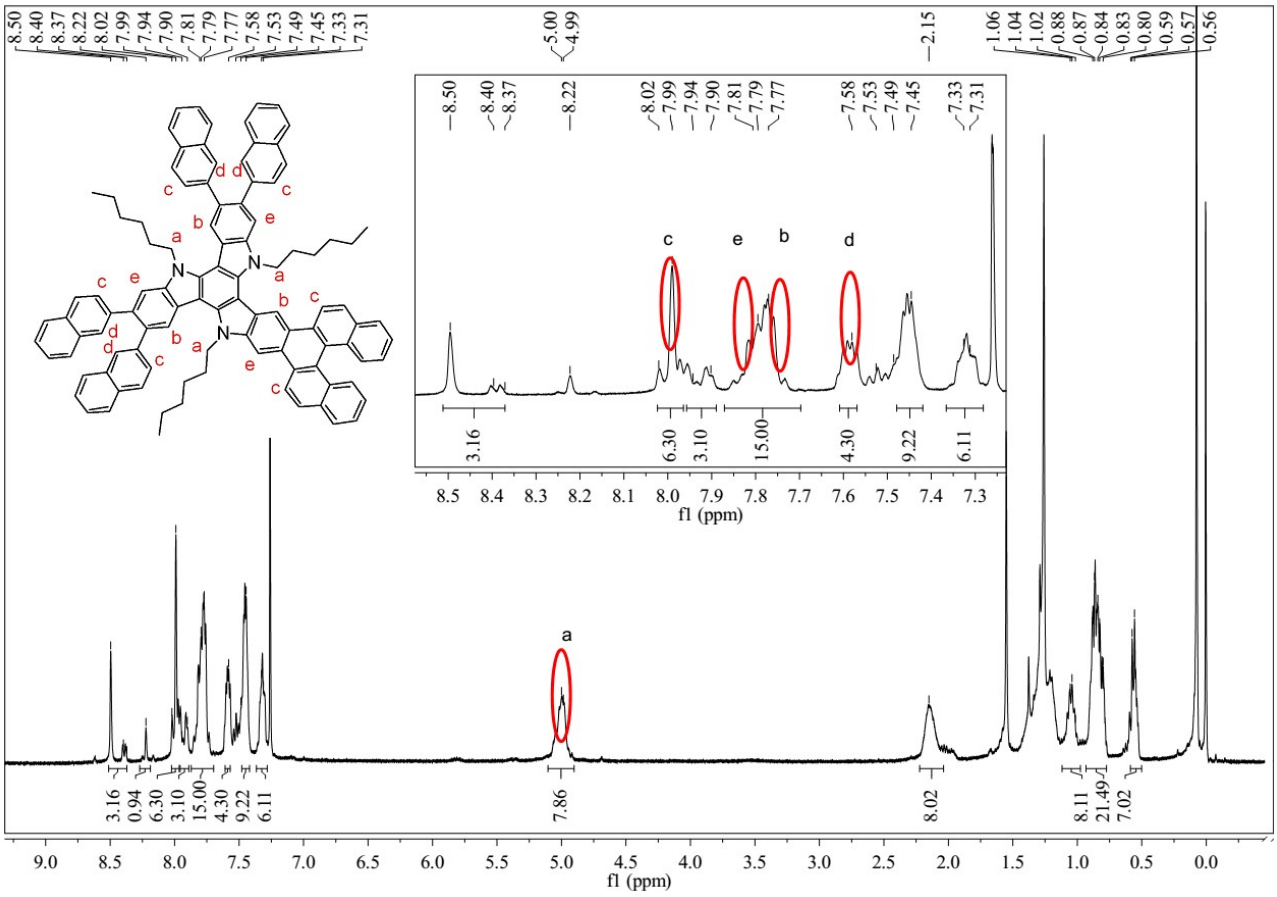

Figure S5. ^{1}H NMR spectra of TATNaC1

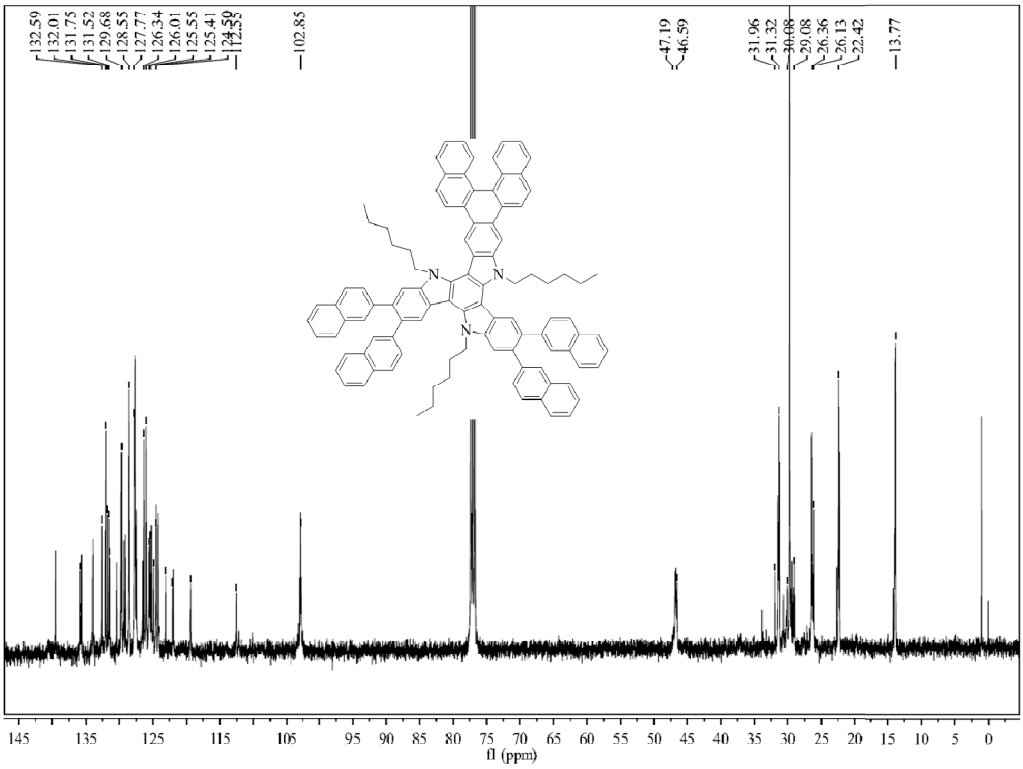

Figure S6. ^{13}C NMR spectra of TATNaC1

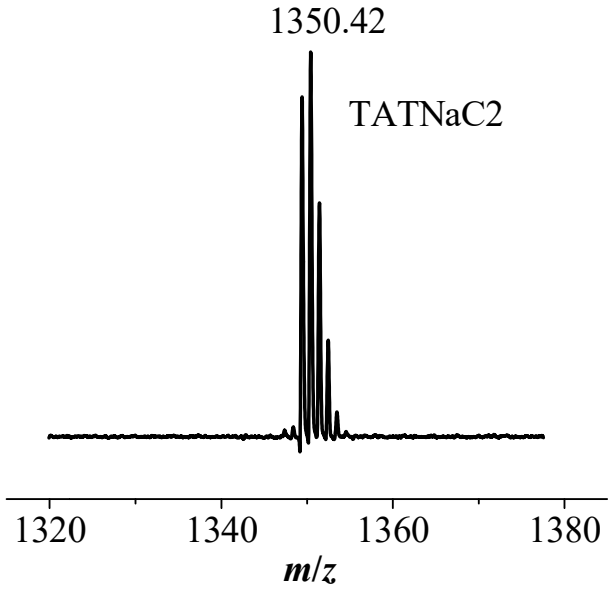

Figure S7. MALDI-TOF MS of TATNaC2

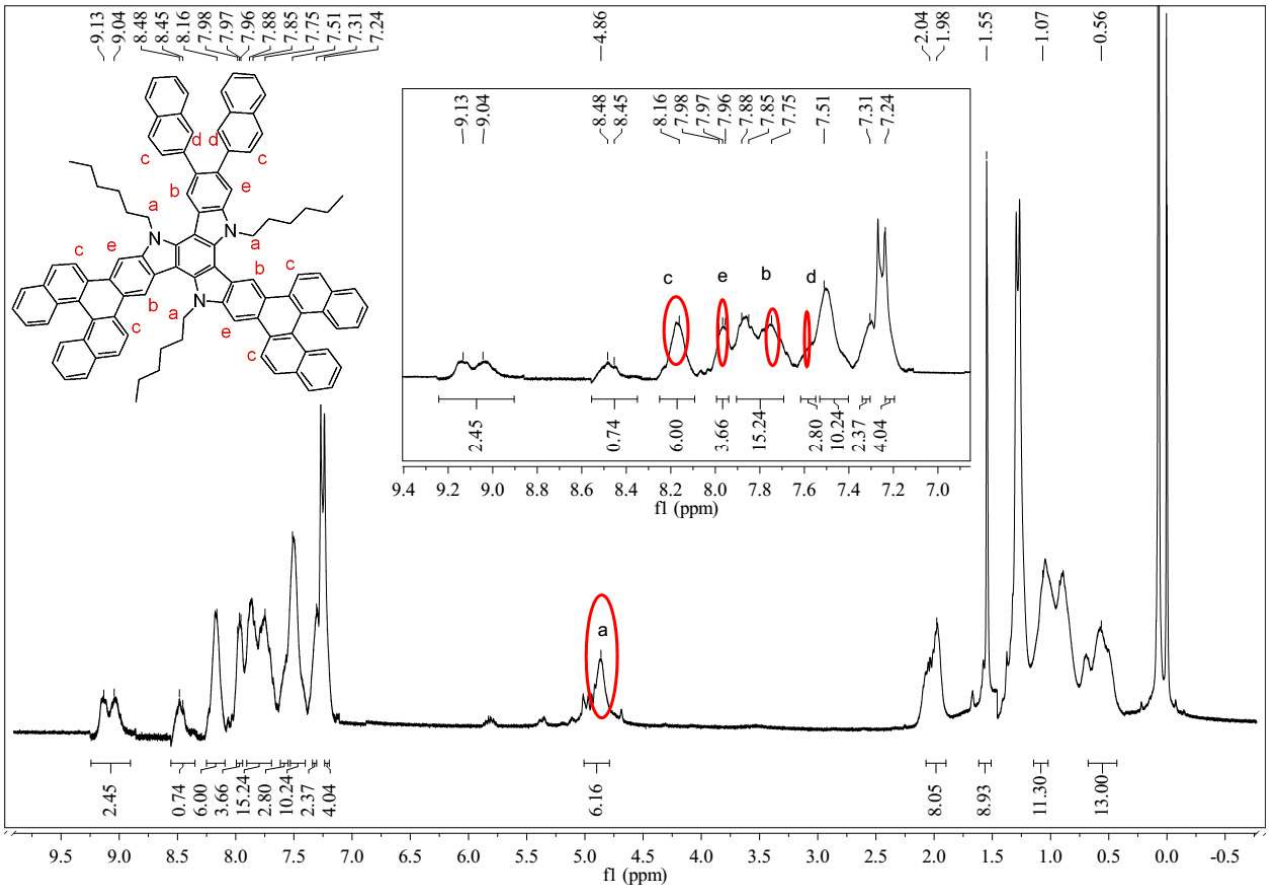

Figure S8. ^{1}H NMR spectra of TATNaC2

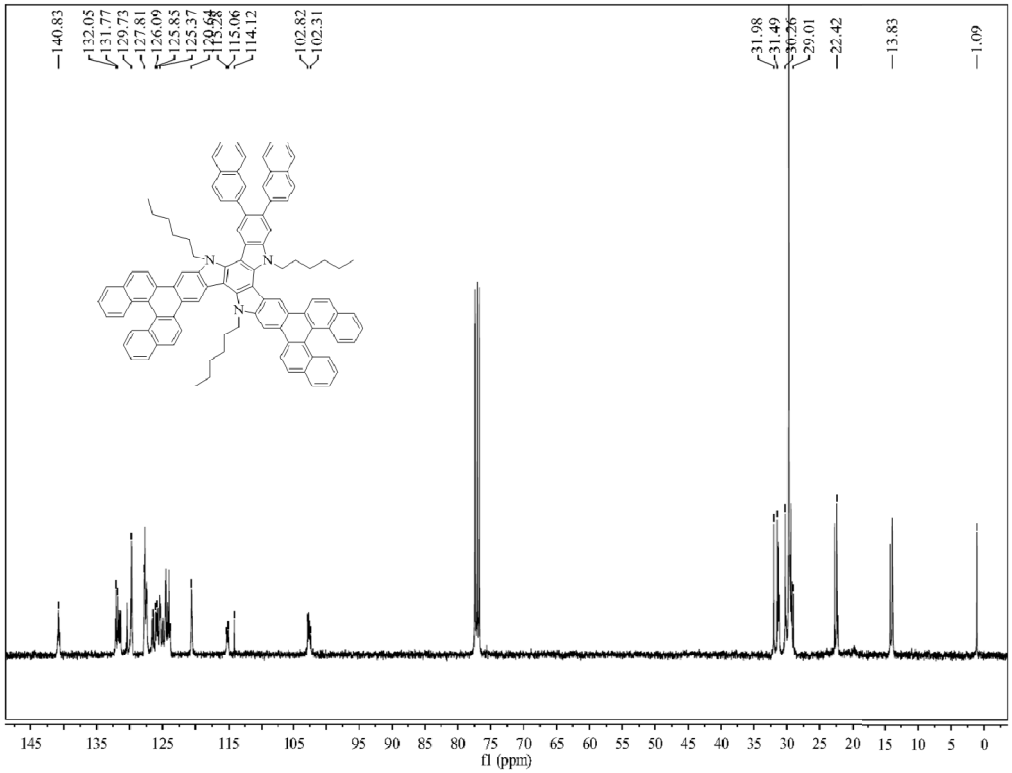

Figure S9. ^{13}C NMR spectra of TATNaC2

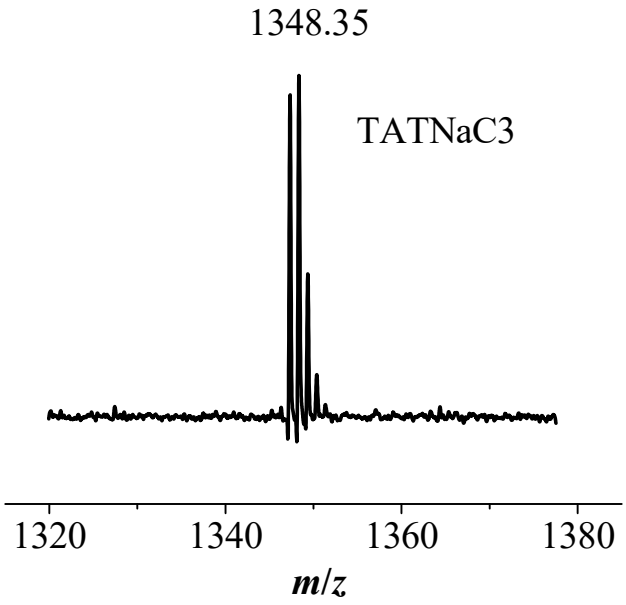

Figure S10. MALDI-TOF MS of TATNaC3

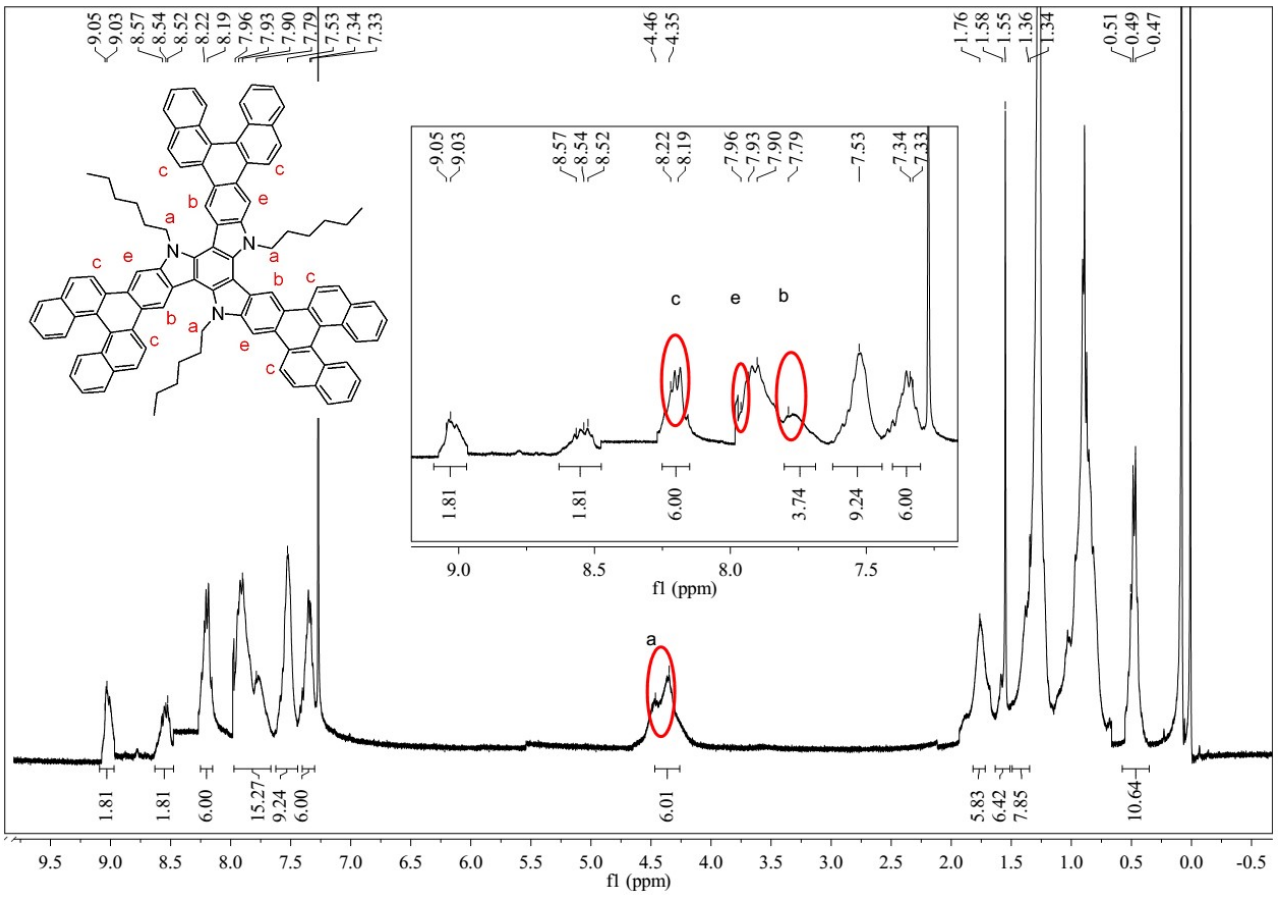

Figure S11. ^{1}H NMR spectra of TATNaC3

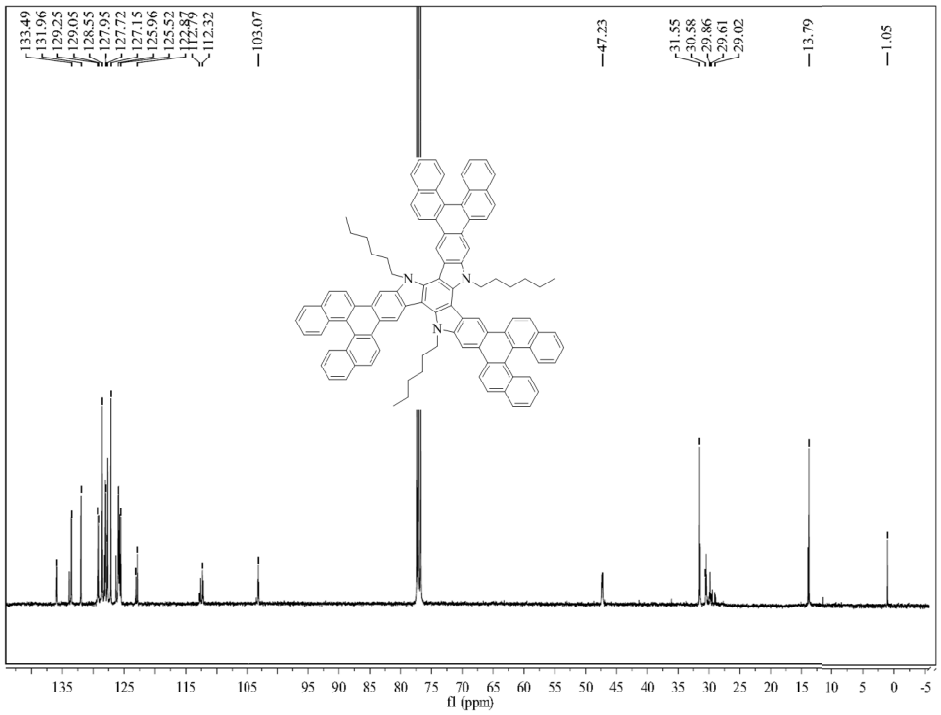

Figure S12. ^{13}C NMR spectra of TATNaC3

Table S1. Eletrochemical Properties of TATNa and TATNaCn.

Compd	λ_{onset} [a] (nm)	E_g^{opt} [b] (eV)	E_{ox} (V)	HOMO (eV)	LUMO (eV)
TATNa	423	2.90	0.58	-5.35[c]/-4.89[d]	-2.45[e]/-1.24[d]
TATNaC1	457	2.70	0.53	-5.30[c]/-4.83[d]	-2.60[e]/-1.43[d]
TATNaC2	467	2.66	0.57	-5.34[c]/-4.84[d]	-2.68[e]/-1.47[d]
TATNaC3	487	2.55	0.58	-5.30[c]/-4.88[d]	-2.75[e]/-1.50[d]

[a] λ_{onset} was the onset for the film absorption spectra. [b] E_g^{opt} (optical energy gap) calculated from the absorption onset of film spectra. [c] Estimated from the onset oxidation and reduction potential by using E_{HOMO} = -[E_{ox}+4.77] eV, $E_{(Fe/Fe+)}$ = 0.03 eV. [d] DFT-calculated results. [e] $E_{LUMO} = E_g + E_{HOMO}$.

References

1. M. J. Frisch, G. W. Trucks, H. B. Schlegel, G. E. Scuseria, M. A. Robb, J. R. Cheeseman, G. Scalmani, V. Barone, B. Mennucci, G. A. Petersson, H. Nakatsuji, M. Caricato, X. Li, H. P. Hratchian, A. F. Izmaylov, J. Bloino, G. Zheng, J. L. Sonnenberg, M. Hada, M. Ehara, K. Toyota, R. Fukuda, J. Hasegawa, M. Ishida, T. Nakajima, Y. Honda, O. Kitao, H. Nakai, T. Vreven, J. A. Montgomery Jr., J. E. Peralta, F. Ogliaro, M. Bearpark, J. J. Heyd, E. Brothers, K. N. Kudin, V. N. Staroverov, T. Keith, R. Kobayashi, J. Normand, K. Raghavachari, A. Rendell, J. C. Burant, S. S. Iyengar, J. Tomasi, M. Cossi, N. Rega, J. M. Millam, M. Klene, J. E. Knox, J. B. Cross, V.

Bakken, C. Adamo, J. Jaramillo, R. Gomperts, R. E. Stratmann, O. Yazyev, A. J. Austin, R. Cammi, C. Pomelli, J. W. Ochterski, R. L. Martin, K. Morokuma, V. G. Zakrzewski, G. A. Voth, P. Salvador, J. J. Dannenberg, S. Dapprich, A. D. Daniels, O. Farkas, J. B. Foresman, J. V. Ortiz, J. Cioslowski and D. J. Fox, Gaussian 09, Revision B.01, Gaussian, Inc., Wallingford, CT, 2010.

2. W.-Y. Lai, R. D. Xia, D. D. C. Bradley and W. Huang, *Chem. Eur. J.* **2010**, *16*, 8471.